

# Studies on the Phase Structure, Mechanical, Rheological Properties, and Nonisothermal Crystallization Kinetics of the Pen/Scf Composites

Li-Juan Zheng,<sup>1</sup> Jian-Gang Qi,<sup>2</sup> Dan Liu,<sup>1</sup> Wen-Feng Zhou<sup>1</sup>

<sup>1</sup>Computer and Information Engineering Department, Shijiazhuang Railway Institute, Shijiazhuang 050043, China

<sup>2</sup>Tian Zheng Supervising Company, Hydrogeology and Engineering Geology of Hebei Prospecting Institute, Shijiazhuang 050021, China

Received 13 June 2008; accepted 6 December 2008

DOI 10.1002/app.29854

Published online 6 March 2009 in Wiley InterScience (www.interscience.wiley.com).

**ABSTRACT:** Short carbon fiber reinforced poly(ethylene 2,6-naphthalate) composites (PEN/SCF) were prepared by twin-screw extruder. The structure, mechanical, rheological properties, and nonisothermal crystallization kinetics of the composites were investigated by scanning electron microscope, universal tester, and differential scanning calorimetry. The results suggest that there is better interaction between SCF and PEN matrix, which leads to an increase in the tensile strength, Young's modulus, and impact strength of the composites with proper contents of SCF. Rheological behavior of the PEN/SCF composites melt is complicated, combining a dilute fluid at lower shear rate and a pseudoplastic fluid at higher shear rate. Moreover, the flow activation energy of the composites suggests that

the melt with more SCF has higher sensitivity to the processing temperature. In conclusion, the composite with 5–10 wt % content of SCF has better properties. The Avrami equation modified by Jeziorny and Ozawa theory was used, respectively, to fit the primary stage of nonisothermal crystallization of various composites. The Avrami exponents  $n$  are evaluated to be 2.6–3.1 for the neat PEN and 3.4–4.8 for PEN/SCF composites, and the SCF served as nucleation agent accelerates the crystallization rate of the composites, and more the content of SCF faster the crystallization rate. © 2009 Wiley Periodicals, Inc. *J Appl Polym Sci* 112: 3462–3469, 2009

**Key words:** poly(ethylene 2,6-naphthalate); SCF; rheology; nonisothermal crystallization

## INTRODUCTION

Compared with the other similar polyesters, poly(ethylene terephthalate) (PET) and poly(butylene terephthalate) (PBT), poly(ethylene 2,6-naphthalate) (PEN) has strong competition because of its excellent properties on the superior thermal, mechanical, barrier, and chemical resistance properties.<sup>1–4</sup> These properties make PEN useful in a wide range of applications, especially in films, magnetic tapes, and packaging materials.<sup>5</sup>

Melt compounding is a straightforward, versatile, and inexpensive method for obtaining new materials with better properties.<sup>6</sup> Jun et al.<sup>7</sup> found that the incorporation of a very small quantity of CNT significantly improved the mechanical property; moreover, it enhanced the crystallization of PEN matrix obviously. Kim and Macosco<sup>8</sup> reported that the highly exfoliated morphology of FGS was maintained in the PEN/FGS composites as revealed by electron microscopy and X-ray scattering, whereas graphite layers remained stacked together even after melt processing.

Our earlier research studied the isothermal crystallization kinetics of PEN/SCF, finding that SCF obviously enhanced the crystallization of PEN matrix.<sup>9</sup>

In practical applications, polymeric materials are usually reinforced with fibers. Because of its good mechanical, thermal, and electrical properties compared with other fiber materials, carbon fibers are widely used in composite production.<sup>10–12</sup> Short carbon fibers (SCFs), in particular, have the additional advantage of being able to be processed using conventional processing techniques, such as extrusion and injection molding.<sup>13</sup>

In this work, the PEN/SCF composites were prepared by twin-screw extruder, and the structure, mechanical, rheological properties, and nonisothermal crystallization kinetics of the composites were investigated by scanning electron microscope (SEM), universal tester, capillary rheometer, and differential scanning calorimetry (DSC), respectively.

## EXPERIMENTAL

### Raw materials

The PEN homopolymer was supplied in pellet form by Honeywell (Minneapolis, MN) with an intrinsic

Correspondence to: L.-J. Zheng (zlj\_hbr@163.com).

viscosity of 0.89 dL/g measured in phenol/tetrachloroethane solution (60/40, w/w) at 30°C. SCF (M40B) used in our experiment was a PAN-based type supplied by Toray Industries (Chiba, Japan) with a diameter of 8  $\mu\text{m}$  and an average length of 4 mm.

### Preparation of composites

PEN was dried in a vacuum oven at 120°C for 4 h and the SCFs were dried in oven at 70°C for 24 h before preparing composites. PEN and SCF were mixed together with different weight ratio of PEN/SCF as following: A0: 100/0; A1: 99/1; A2: 98/2; A3: 95/5; A4: 90/10, and then melt-blended in a ZSK-25WLE (Stuttgart, Germany, WP) self-wiping, corotating twin-screw extruder operating at a screw speed of 100 rpm and at a die temperature of 300°C. The resultant composite ribbons were cooled in cold water, cut up, and redried before being used in measurements.

### Mechanical properties test

Tensile properties were determined at room temperature on the Universal Testing Machine (Model 1130, Instron Corporation, Houston, TX) at the crosshead speed of 50 mm/min (ASTM D638). The notched Izod impact strength was measured on the impact tester (Sumitomo, Tokyo, Japan; ASTM D256).

### Structural performance characterization

The phase structure of the fracture surface of the impacted samples, after coating with a thin layer of gold, was investigated by KYKY-2800B type scanning electron microscope (Travor-Norther Co., USA) at an accelerating voltage of 25 kV.

### Rheological performance characterization

The rheological measurements were performed on a LY-II type capillary rheometer (Jilin University, China) at the temperature of 280°C, 285°C, 290°C, and 295°C, respectively. The 1.5 g sample was put into the capillary at thermostatic temperature, held for 10 min, and then measured at the shear stress range of 6.5–75.5 kPa.

### Differential scanning calorimetry

The nonisothermal crystallization behaviors were performed on the Perkin-Elmer Diamond DSC instrument that calibrated with indium before performing the measurement and the weights of all samples were approximately 6.0 mg. The sample was heated to 300°C in nitrogen, held for 5 min and

then cooled to 30°C at constant cooling rates of 5, 10, 15, 20, 30, 40°C/min, respectively. The exothermic curves of heat flow as a function of temperature were recorded and investigated.

## RESULTS AND DISCUSSION

### Phase structure

Figure 1 shows the SEM images of the fracture surface: (a) neat PEN, (b) PEN/SCF 95/5, and (c) part

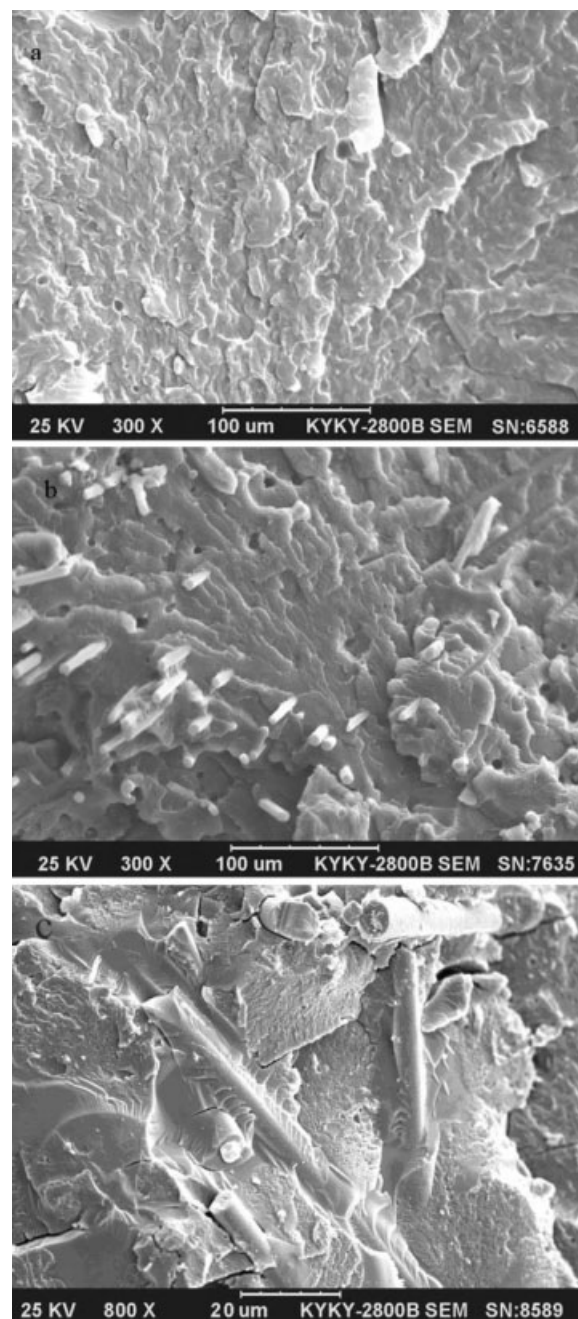


**Figure 1** SEM micrographs of fracture surface of neat PEN (a), the PEN/SCF 95/5 (b), and part enlarged of PEN/SCF 95/5 (c).

**TABLE I**  
**Mechanical Properties of PEN/SCF Composites**

SCF (wt %)	$\sigma_t$ (MPa) <sup>a</sup>	$\sigma_b$ (MPa) <sup>b</sup>	$E$ (MPa) <sup>c</sup>	$\sigma_i$ (kJ/m <sup>2</sup> ) <sup>d</sup>
0	48.4	35.6	1813.3	7.5
1	61.5	39.8	2000.4	8.9
2	79.2	45.7	2099.3	9.2
5	101.1	50.8	2212.9	10.5
10	108.7	58.1	2398.2	8.8

<sup>a</sup> Tensile strength.

<sup>b</sup> Break strength.

<sup>c</sup> Young's modulus.

<sup>d</sup> Impact strength.

enlarged of PEN/SCF 95/5. It can be seen that the fracture surface of neat PEN is smooth, whereas the fracture surface of PEN/SCF 95/5 is relative rough and some SCFs are randomly dispersed in the matrix resin. Separation occurred when impact, but the SCF surface is enwrapped with a mass of PEN resins. These phenomena suggest that the SCF and the resin have a better interaction.<sup>14,15</sup> The ruptured energy is expended on fiber fracture, fiber pull-out, fiber and the matrix debonding. It can deduce that the mechanical properties of the composites will profit from the interface adherence.

### Mechanical properties

The mechanical properties of the polymer composites are remarkably influenced by the SCF and it can be obtained through changing the component of the composites. The influence of the SCF content on the tensile strength and notched Izod impact strength of composite are listed in Table I. When the content of SCF is 0–10 wt %, the tensile strength ( $\sigma_t$ ), break strength ( $\sigma_b$ ), and  $E$  are increased as a function of SCF content. When the SCF content is 2–5 wt %, the tensile strength of PEN/SCF composites is twice more as much as that of neat PEN. When the SCF content is 5–10%, the tensile strength increases slowly and the reinforcement effect goes to saturation. This result is because the distribution state of SCF in composites changes gradually from single to overlap each other with the content of SCF increases, which is helpful for stress transfer and carrying capacity; as a result, the tensile strength is enhanced largely when the SCF content is increased from 2 to 5 wt %. However, the reinforcement effect approaches to saturation when the overlapped structure is up to saturation, so the tensile strength increases slowly when the SCF content is 5–10%.

The impact energy is usually expended on fiber fracture, fiber pull-out, fiber and the matrix debonding, the formation of the new surface, and the plastic deformation. The Izod impact strength ( $\sigma_i$ ) is

improved obviously, which increased by 40% as comparison with neat PEN when the SCF content is 5 wt %, and then decreases when the SCF content is more than 5 wt %. The reason is when the SCF content is less than 5 wt %, the reinforcement effect can lead to the crack propagation path to become longer, with the fiber drawn from the polymeric matrices playing a main role, and this effect is helpful for energy absorption. However, when the SCF content is more than 5 wt %, too much SCFs make the chains of PEN hard to move, the reinforcement effect will be weak although the inner crack effects initiated by SCFs are strong, which leads to the crack propagation path to become shorter and restrains energy absorption.<sup>16</sup> These results suggest that the incorporation of SCF significantly improves the mechanical properties of PEN. It should be noted that, for the sake of composites has both the rigidity and the toughness, the SCF content in range of 5–10 wt % will be better.

### Rheological behavior

The Hagen-Poiseuille equation

The melt apparent viscosity  $\eta_a$  is defined by the Hagen-Poiseuille equation<sup>16</sup> as the following formula:

$$\eta_a = \pi \Delta P R^4 / 8QL \quad (1)$$

where  $\Delta P$  is the measured pressure drop,  $R$  is the radius of capillary,  $L$  is the length of capillary, and  $Q$  is the flow volume of liquid. The ratio of  $L/D$  of rheometer is 40 : 1, so that the flow of melt can be regarded as steady flow under lower shear stress and the end effecting can be ignored.

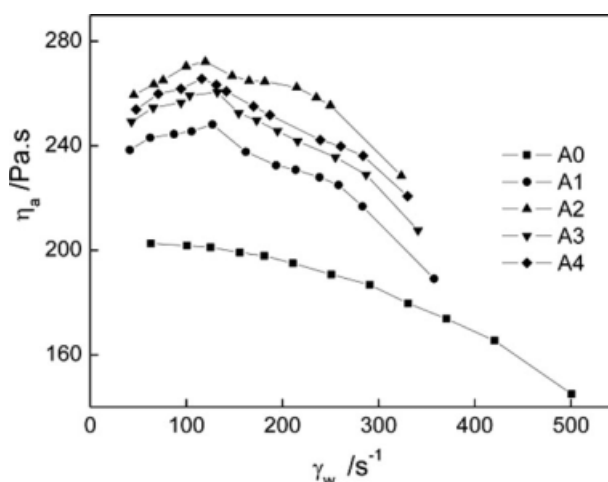


**Figure 2** Relationship between apparent viscosity and shear rate of different composites at 285°C.

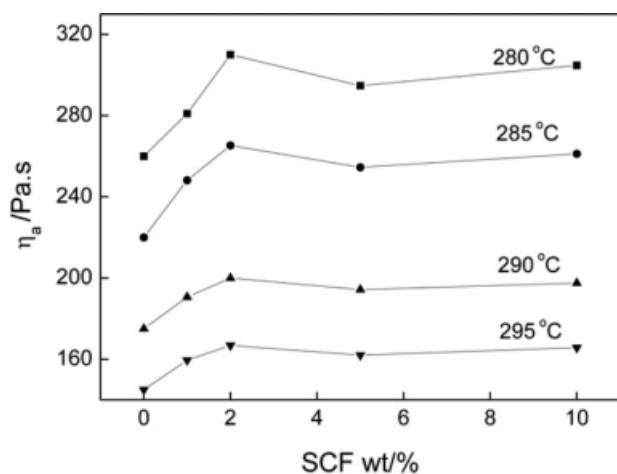


**Figure 3** Relationship between  $\eta_a$  and SCF content in composites at different temperatures.

The shear stress ( $\tau_w$ ) is defined as:

$$\tau_w = \Delta PR/2L \quad (2)$$

The shear rates ( $\dot{\gamma}_w$ ) is defined as:

$$\dot{\gamma}_w = -dv/dr = 4Q/\pi R^3 \quad (3)$$

Melt apparent viscosity, shear stress, and shear rate are calculated by eqs. (1)–(3). Figure 2 shows the rheological curves of different liquid at 285°C in the form of the plot of apparent viscosity versus shear rate. It is seen that the melt viscosity of neat PEN decreases gradually with the shear rate increasing from 30 to 500  $s^{-1}$ ; thus, the phenomenon of shearing-thickening occurs and PEN melt is pseudo-plastic liquid.

However, the PEN/SCF composites have complicated rheological behaviors. The samples of PEN/SCF 99/1, 98/2, 95/5, and 90/10 all have maximum viscosity and then the melt viscosity decreases gradually as the shear rate increasing from 30 to 500  $s^{-1}$ . Moreover, the viscosity data of all composites are all higher than that of neat PEN. The reason is the SCF collide each other under lower shear rate, so some SCF may overlap each other at the beginning of the flowing stage, which induces the melt viscosity increased. When the shear rate is up to a certain value, the overlapped structure is destroyed and the SCF starts to tropism; moreover, the losing of the tied points between polymer chains becomes easy under high shear rate. Thus, the melt viscosity decreases gradually as the shear rate increases unceasingly.

At different temperatures, the melt apparent viscosity versus the SCF content is plotted in Figure 3. It is clear that the melt viscosity of each sample decreases with increasing temperature from 280 to 295°C, indicating that increasing temperature can

improve the material processing. However, different melt has different sensitivity to temperature.

Arrhenius equation

The Arrhenius equation<sup>17</sup> can be used to illustrate the dependence of the melt apparent viscosity ( $\eta_a$ ) on temperature, that is

$$\ln \eta_a = \ln A + (\Delta E_\eta/RT) \quad (4)$$

where  $\Delta E_\eta$  is the viscous activation energy,  $A$  is the pre-exponent factor, and  $R$  is the gas constant. By drawing the plot of  $\ln \eta_a$  versus  $1/T$ , a straight line is obtained, and  $\Delta E_\eta$  can be derived from the slope of line.

Viscous activation energy  $\Delta E_\eta$  is the least energy that the moving unit of the chain needed to conquer the vallum and remove to the next hole nearby.  $\Delta E_\eta$

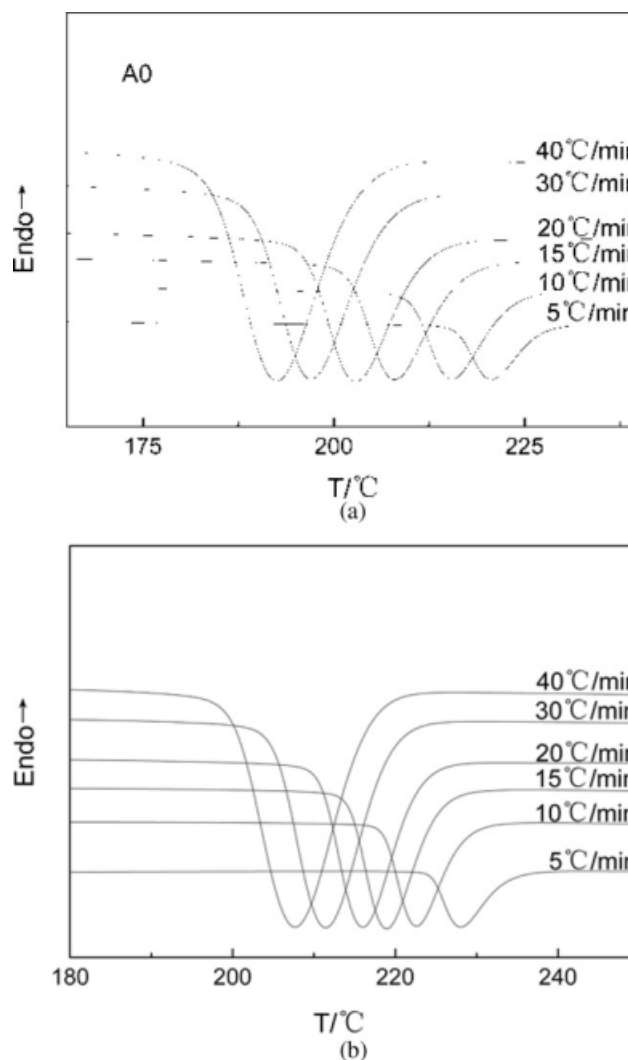


**Figure 4** Nonisothermal crystallization curves of (a) A0 and (b) A4 composites at different cooling rates.

**TABLE II**  
Nonisothermal Crystallization Kinetic Parameters of A0, A1, and A4 by Jeziorny Equation

$D$ (°C/min)	$T_{cp}$ (°C)	$n$	$t_{1/2}$ (min)	$K_c$ ( $10^{-4} \text{ s}^{-n}$ )	$\Delta H_c$ (J/g)	
A0	5	220.6	3.1	6.4	94	-41.1
	10	212.6	3.0	4.6	116	-40.0
	15	206.1	2.9	3.8	168	-37.2
	20	200.4	2.8	3.5	241	-33.6
	30	196.3	2.7	3.2	327	-24.8
	40	191.5	2.6	2.9	473	-21.9
A1	5	229.7	4.2	4.3	295	-40.1
	10	218.7	3.9	3.7	510	-39.1
	15	215.9	3.8	3.1	600	-38.2
	20	211.8	3.7	2.8	720	-36.0
	30	206.1	3.6	2.6	830	-35.6
	40	202.9	3.4	2.4	1010	-34.4
A4	5	230.0	4.8	4.2	596	-38.1
	10	222.6	4.4	3.5	946	-36.6
	15	219.0	4.3	3.0	1144	-36.4
	20	216.0	3.7	2.5	1687	-35.6
	30	211.4	3.7	2.3	1890	-35.4
	40	209.7	3.5	2.1	2922	-33.6

values calculated from the eq. (4) for neat PEN and PEN/SCF 99/1, 98/2, 95/5, and 90/10 are 25.0, 29.0, 32.1, 31.5, and 30.8 kJ/mmol, respectively. The neat PEN has the lowest  $\Delta E_\eta$  value, the reason is the chain of PEN moving embarrass due to the addition of SCF.

#### Nonisothermal crystallization kinetics analysis

Analysis based on the Avrami theory modified by Jeziorny

The relative crystallinity ( $X_t$ ) as a function of temperature is defined as the following equation:

$$X_t = \frac{\int_0^t (dH/dt)dt}{\int_0^\infty (dH/dt)dt} \quad (5)$$

where the  $dH/dT$  is the rate of heat evolution,  $t_0$  and  $t_\infty$  are the time, at which crystallization starts and ends, respectively.

The relationship between temperature  $T$  and time  $t$  is given by eq. (6) during the nonisothermal crystallization process, as follows:

$$t = \frac{|T_0 - T|}{D} \quad (6)$$

where  $t$  is the crystallization time,  $T_0$  is the temperature at which crystallization begins ( $t = 0$ ),  $T$  is the temperature at a crystallization time  $t$ , and  $D$  is the cooling rate.

The nonisothermal crystallization exothermic peaks of A0 and A4 composites at various cooling rate are shown in Figure 4, and their parameters are summarized in Table II. The exothermic peak tem-

perature,  $T_{cp}$ , shifts to lower temperature region with increasing cooling rates from 5 to 40°C/min. From the DSC digital information,  $X_t$  is calculated at different temperature and time, and the plots of  $X_t$  versus  $t$  are shown in Figure 4(a,b).

It can be seen from Figure 4 that all these curves have similar sigmoid shape, and the curvature of the upper parts of the plot is observed to be level off due to the spherulites impingement that already begin from the inflection point of the curves. The characteristic sigmoid curves are shifted to lower temperature or shorter time with increasing cooling rates for completing the crystallization. Through Figure 5(a,b), we can get the half-time of crystallization,  $t_{1/2}$ , when the  $X_t$  is equal to 50%, and the parameters are listed in Table II. It can be seen that  $t_{1/2}$  values decrease with increasing cooling rates, indicating a faster crystallization rate with increasing cooling rate. Moreover, compared the values of  $t_{1/2}$  of A0 with those of A1 and A4 at a given cooling rate, it is clear that the SCF accelerates the

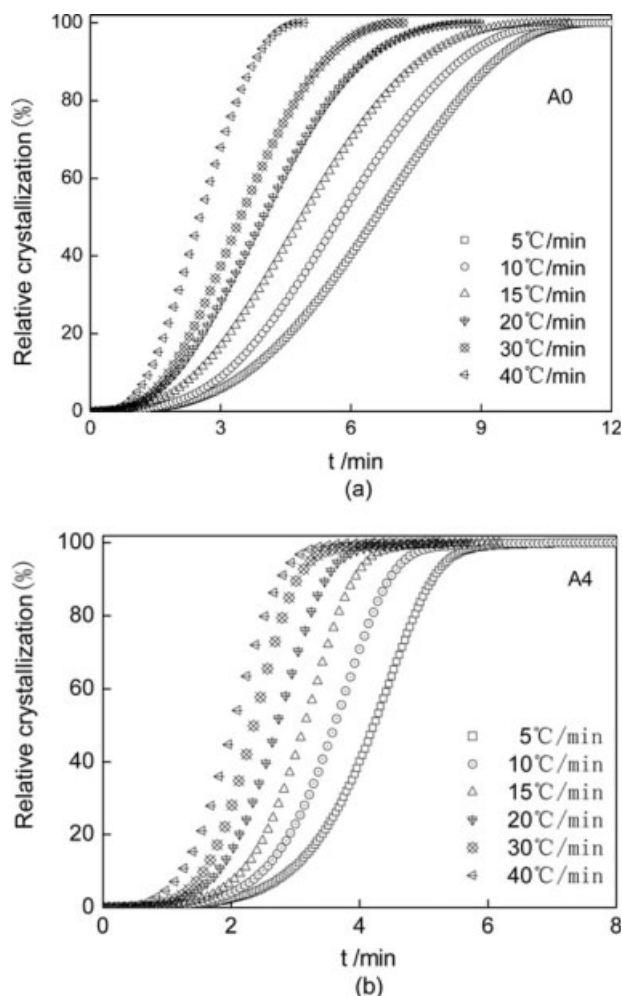


**Figure 5** Relative crystallization versus time for nonisothermal crystallization of (a) A0 and (b) A4 composites.

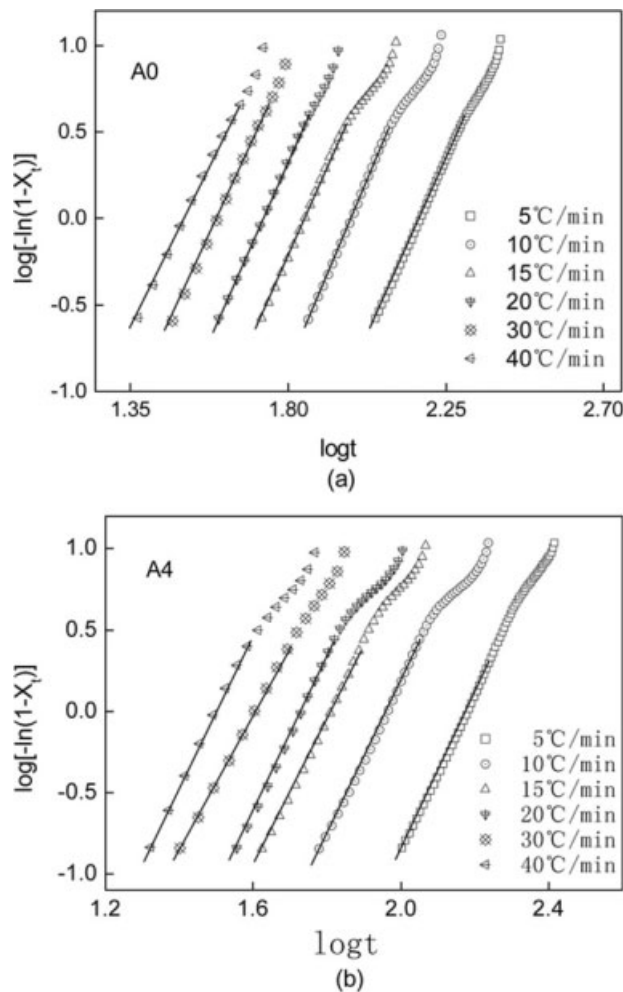


**Figure 6** Plots of  $\log[-\ln(1 - X_t)]$  versus  $\log t$  for nonisothermal crystallization of (a) A0 and (b) A4 composites.

crystallization rate of PEN, and more the SCF component in composites higher the crystallization rate.

The primary stage of nonisothermal crystallization could be described by Avrami equation,<sup>18,19</sup> based on the assumption that the crystallization temperature is constant; it can be obtained the following:

$$1 - \dot{X}_t = \exp(-K_t t^n) \tag{7}$$

$$\log[-\ln(1 - X_t)] = n \log t + \log K_t \tag{8}$$

where  $K_t$  is a growth rate constant involving both nucleation and growth rate parameters. Jeziorny<sup>20</sup> considered the values of  $K_t$  determined by Avrami equation should be adequate as follows:

$$\log K_c = \frac{\log K_t}{|D|} \tag{9}$$

where  $K_c$  is the kinetic crystallization rate constant.

Figure 6(a,b) shows a series of double logarithm plots of  $\log[-\ln(1 - X_t)]$  versus  $\log t$  at different cooling rates. Each curve in Figure 6 shows good lin-

earity except a secondary crystallization at the later crystallization stage. The Avrami exponent  $n$  and  $K_c$  of A0, A1 and A4 obtained from the slopes and the intercepts are listed in Table I, respectively.

The Avrami exponent,  $n$ , is found to range from 3.1 to 2.6 for PEN, from 4.2 to 3.4 for A1, and from 4.8 to 3.5 for A4 when cooling rates increase from 5 to 40 °C/min. The values of  $n$  decrease with increasing cooling rate for each sample gradually, which indicates a fewer dimensions crystallization growth.<sup>21-23</sup> Judged from the  $n$  of neat PEN, its nucleation type should predominantly by homogeneous thermal nucleation and its crystal growth should dominantly change from three-dimensional to two-dimensional crystal growth with increasing cooling rate. However, for A1 and A4 with heterogeneous nucleus, the values of exponent  $n$  are between 3.4 and 4.8 at various cooling rates, which is not consist with the supposing of the Avrami theory. This result may due to the spherulites' impingement and crowding, or the complicated nucleation types and growth form of spherulites. And it is known that the nucleation mode is dependent on the cooling rate. So its nucleation type should mostly be a heterogeneous nucleation and its crystal growth dimension should mostly be three-dimensional space extension.<sup>24</sup>

It can be clearly seen in Table II that  $K_c$  increases as a function of  $D$ , and PEN/SCF composites have a higher value of  $K_c$  than that of pure PEN at a given cooling rate. These results suggest that the crystallization rate is accelerated greatly with the addition of SCF, and more the SCF content in composites higher the crystallization rate. Moreover,  $\Delta H_c$  of each sample is gradually decreased due to the less amorphous polymer turned into crystal form in the composite with increasing cooling rate. At the same cooling rate,  $\Delta H_c$  of A0, A1, and A4 is decreasing with increasing content of SCF in composites, indicating that the crystalline formation is decreased by the SCF.

#### Analysis based on the Ozawa theory

As the nonisothermal crystallization is a rate-dependent process, Ozawa<sup>25</sup> took into account the effect of cooling (or heating) rate,  $D$ , on the crystallization process from the melt or glassy state, and modified the Avrami equation as follows:

$$1 - X_t = \exp\left[-\frac{K(T)}{|D|^m}\right], \tag{10}$$

$$\log[-\ln(1 - X_t)] = \log K(T) - m \log|D| \tag{11}$$

where  $K(T)$  is a function related to the overall crystallization rate that indicates how fast crystallization

proceeds, and  $m$  is the Ozawa exponent that depends on the dimension of crystals growth. According to the Ozawa's theory and plots of  $\log[-\ln(1 - X_t)]$  versus  $\log|D|$  at a given temperature, a series of straight lines will be obtained if Ozawa analysis is valid, and the crystallization kinetic parameters  $m$  and  $\log K(T)$  can be derived from the slope and the intercept, respectively.

The results of the Ozawa analysis for A0 and A4 composites are shown in Figure 7(a,b), and a series of straight lines are obtained, and the values of  $m$  and  $\log K(T)$  are listed in Table III. For each composite, the values of  $m$  and  $\log K(T)$  are increased with the increasing temperature indicating that the crystallization growth is on more dimensions and at fast crystallization rate at the higher temperature, whereas it is on less dimensions and lower crystallization rate at the lower temperature.<sup>26</sup> Furthermore, comparing the values of  $m$  and  $\log K(T)$  of A0 with those of A1 and A4 in the temperature range of 200

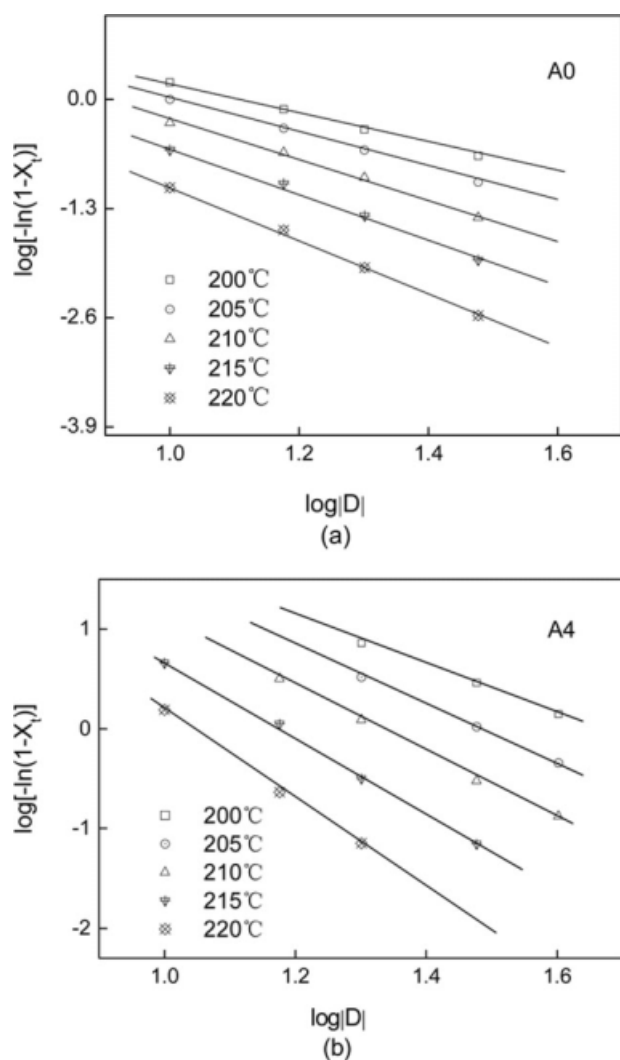


**Figure 7** Ozawa plots of  $\log[-\ln(1 - X_t)]$  versus  $\log|D|$  for (a) A0 and (b) A4 composites.

**TABLE III**  
Nonisothermal Crystallization Kinetic Parameters of A0, A1, and A4 Analyzed by Ozawa Equation

$T$ ( $^{\circ}\text{C}$ )	A0		A1		A4	
	$m$	$\log K(T)$	$m$	$\log K(T)$	$m$	$\log K(T)$
200	1.7	1.90	2.7	3.82	2.8	3.99
205	2.0	1.91	2.9	4.14	2.9	4.26
210	2.3	1.95	3.2	4.36	3.5	4.51
215	2.6	2.01	3.6	4.43	4.1	4.59
220	2.8	2.05	4.4	4.54	4.7	4.63

to  $220^{\circ}\text{C}$ , it is obvious that the results of A0 are much lower than those of A1 and A4, indicating that SCF can accelerate crystallization rate of PEN, and more the SCF content in composites higher the crystal growth dimension and the crystallization rate.

## CONCLUSIONS

In this work, a systematic study on the PEN/SCF composites has been carried out. The SCF has better interaction with the PEN resin, which lead to the improved tensile and impact strength of the composite with proper content of SCF. PEN/SCF composites melt have complicate rheological behaviors, i.e., dilated fluid at lower shear rate and pseudoplastic fluid at higher shear rate. Moreover, the viscous activation energy increases first and then decreases as the content of SCF increases, implying that the melt with SCF has higher sensitivity to the processing temperature. Combining the results of mechanical and other properties, the appropriate content of SCF in composites is in range of 5–10 wt %. The Avrami equation modified by Jeziorny and Ozawa theory were used, respectively, to fit the primary stage of nonisothermal crystallization of various composites. The results indicate that composites with proper content of SCF show relative higher crystallization temperature, crystallization rate, and crystallinity than the neat PEN because the SCF has served as nucleation agent for PEN.

## References

- Shin-Ichiro, I.; Masayoshi, I. *J Appl Polym Sci* 2008, 110, 1814.
- Schoukens, G.; Clerck, K. D. *Polymer* 2005, 46, 845.
- George, P. K.; Nickolaos, P.; Dimitris, N. B.; George, Z. P. *Polymer* 2003, 44, 7801.
- Pongpipat, K.; Pitt, S. *Eur Polym J* 2005, 41, 1561.
- Kaynak, C.; Orgun, O.; Tincer, T. *Polym Test* 2005, 24, 455.
- Lee, W. D.; Yoo, E.; Im, S. S. *Polymer* 2003, 44, 6617.
- Jun, Y. K.; Sang, H.; Seong, H. K. *Polym Eng Sci* 2007, 47, 1715.
- Kim, H.; Macosco, C. W. *Macromolecules* 2008, 41, 3317.
- Zheng, L. J.; Qi, J. G.; Zhang, Q. H.; Zhou, W. F.; Liu, D. *J Appl Polym Sci* 2008, 108, 650.
- Malchev, P. G.; Davidc, C. T.; Picken, S. J.; Gotsis, A. D. *Polymer* 2005, 46, 3895.

11. Crowson, R. J.; Folkes, M. J. *Polym Eng Sci* 1980, 20, 934.
12. Gullu, A.; Ozdemir, A.; Ozdemir, E. *Mater Design* 2006, 27, 316.
13. Varatharajan, R.; Malhotra, S. K.; Vijayaraghavan, L.; Krishnamurthy, R. *Mater Sci Eng B* 2006, 132, 134.
14. Li, C.; Liu, X. B. *Mater Lett* 2007, 61, 2239.
15. He, F. *Carbon Fiber and Applications*; Bei Jing, 2004.
16. Zhang, G.; Thompson, M. R. *Compos Sci Technol* 2005, 65, 2240.
17. Burkus, Z.; Temelli, F. *Carbohydr Polym* 2005, 59, 459.
18. Qiu, Z. B.; Yang, W. T. *Polymer* 2006, 47, 6429.
19. Qiu, Z. B.; Yang, W. T. *J Appl Polym Sci* 2007, 104, 972.
20. Jeziorny, A. *Polymer* 1978, 19, 1142.
21. Qiu, Z. B.; Yang, W. T. *J Appl Polym Sci* 2006, 102, 4775.
22. Guan, Y.; Wang, S. Z.; Zheng, A. N.; Xiao, H. N. *J Appl Polym Sci* 2003, 88, 872.
23. Lu, M.; Ye, L.; Mai, Y. W. *Comp Sci Technol* 2004, 64, 191.
24. Huang, H.; Gu, L. X.; Ozaki, Y. *Polymer* 2006, 64, 104.
25. Ozawa, T. *Polymer* 1971, 12, 150.
26. Yuan, Q.; Awate, S.; Misra, R. D. K. *Eur Polym J* 2006, 42, 1994.